Turbine Blade Cooling System Optimization

Julian Girardeau, Jérôme Pailhes, Patrick Sebastian, Frédéric Pardo, Jean-Pierre Nadeau

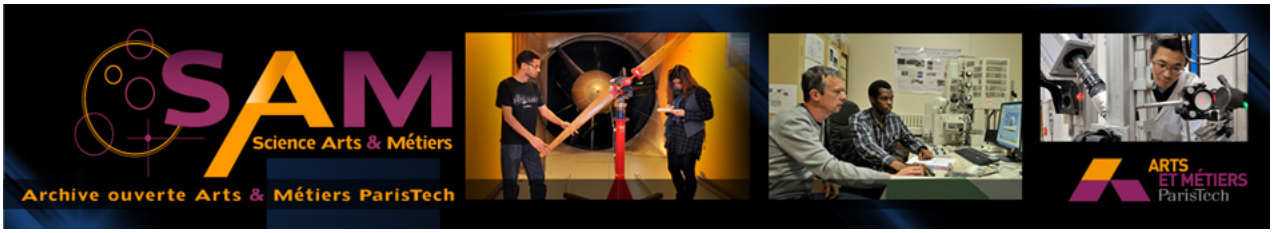

Julian Girardeau
Arts et Metiers ParisTech,
I2M, UMR 5295,
Talence F-33400, France;
TURBOMECA SAFRAN Group,
Bordes F-64511, France
e-mail: julian.girardeau@snecma.fr

Jérôme Pailhes[1]
Arts et Metiers ParisTech,
I2M, UMR 5295,
Talence F-33400, France
e-mail: jerome.pailhes@ensam.eu

Patrick Sebastian
Univ. Bordeaux,
I2M, UMR 5295,
Talence F-33400, France
e-mail: patrick.sebastian@i2m.u-bordeaux.fr

Frédéric Pardo
TURBOMECA SAFRAN Group,
Bordes F-64511, France
e-mail: frederic.pardo@turbomeca.fr

Jean-Pierre Nadeau
Arts et Metiers ParisTech,
I2M, UMR 5295,
Talence F-33400, France
e-mail: jean-pierre.nadeau@ensam.eu

Turbine Blade Cooling System Optimization

Designing high performance cooling systems suitable for preserving the service lifetime of nozzle guide vanes of turboshaft engines leads to significant aerodynamic losses. These losses jeopardize the performance of the whole engine. In the same time, a low efficiency cooling system may affect the costs of maintenance repair and overhaul of the engine as component life decreases. Consequently, designing cooling systems of gas turbine vanes is related to a multiobjective design problem. In this paper, it is addressed by investigating the functioning of a blade and optimizing its design by means of an evolutionary algorithm. Systematic 3D CFD simulations are performed to solve the aerothermal problem. Then, the initial multiobjective problem is solved by aggregating the multiple design objectives into one single relevant and balanced mono-objective function; two different types of mono-objective functions are proposed and compared. This paper also proposes to enhance available knowledge in the literature of cooling systems of gas turbine vanes by simulating the internal cooling system of the vane. From simulations thermal efficiency and aerodynamic losses are compared and their respective influences on the global performances of the whole engine are investigated. Finally, several optimal designs are proposed. [DOI: 10.1115/1.4023466]

Keywords: nozzle guide vanes, cooling systems, multiobjective optimization, aggregation

1 Introduction

For decades, turbine designers try to increase mean turbine inlet temperatures (hereafter denoted T_{41}) to increase the performances of new turboshaft engine generations. Indeed, this temperature tremendously influences the performances of turboshaft engines based on Joule–Brayton thermodynamic cycles and, more especially, both the available power at the output of the system and its thermal efficiency.

In order to decrease engine operating costs, turbine designers must also increase their component lifetimes. However, high gas temperature levels throughout the engine require more cooling air or better cooling efficiency to protect parts from thermal damage. One of the element with potentially the greatest exposure to thermal damage is the high pressure turbine nozzle guide vane (NGV) downstream of the combustion chamber. Designing high performance cooling systems able to preserve the lifetime of this component can lead to significant aerodynamic losses, which degrades aerodynamic characteristics of the gas flow circulating through the vane. These losses next degrade energetic performances in the first turbine stage and; consequently, those of the whole engine. In particular, the specific fuel consumption and specific power of the turboshaft engine respectively increase or decrease. Designers therefore have to search for solutions satisfying antagonist objectives and maximizing several performance indicators such as cooling efficiency or high pressure turbine stage efficiency.

Müller [1], Nowak [2,3] and Morrone [4] have already studied and optimized cooling systems of gas turbine vanes by means of evolutionary algorithms. But, according to the authors, these preceding publications do not consider the whole internal cooling system of a blade in a 3D aerothermal CFD simulation or do not compare thermal efficiency performances with aerodynamic losses and their influence on the whole engine efficiency. Indeed, Nowak [2] considered a vane cooled with radial tubes and aimed at minimizing both mean and maximum metal temperatures of the vane, without taking into account impingement cooling or film cooling as being design variables. Further works related to this problem [3] introduce a new objective function aiming at reducing both metal temperatures and thermal stresses but the influence of the cooling gas flow was still not considered. Muller and Morrone [1,4] introduce film cooling and impingement cooling parameters when considering 2D vanes. Their objective functions were built to minimize both metal temperature and coolant mass flow. However, as discussed later in this paper and in Ref. [5], the coolant mass flow is not, sufficient to determine turbine stage efficiency. For instance, the use of film cooling acts on aerodynamic losses depending on where leakage areas are located along the chord of the vane blades.

In this paper, enhancements of these previous works are introduced. High pressure turbine stage efficiency change with the vane design will be quantified and taken into account within new objectives functions. Cooling devices thermal efficiencies will be estimated according to 3D CFD simulations and combined into a single model with coolant mass flows, heat transfer rates, metal and fluid temperature estimations. Finally, design choices influencing the whole engine design are considered in a comprehensive and balanced manner, leading to more relevant satisfactions of the objectives. This approach is facing with several difficulties and challenges entailing:

- the management of high computation times and topology changes within a 3D CFD model

[1]Corresponding author.

Contributed by the International Gas Turbine Institute (IGTI) of ASME for publication in the JOURNAL OF TURBOMACHINERY. Manuscript received August 29, 2012; final manuscript received November 29, 2012; published online September 13, 2013. Editor: David Wisler.

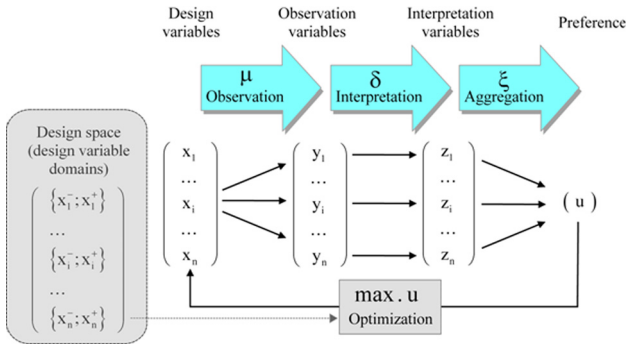

Fig. 1 The OIA flow chart

- the combination of multiobjective performance criteria into a well-balanced objective function
- the complexity of the model linking physical phenomena to the functioning of the whole engine and to design objectives

These difficulties are addressed in this paper by developing two different models from the observation-interpretation-aggregation (OIA) method proposed in Refs. [6] and [7]. These two models differ in the interpretation and aggregation functions. In the second paragraph of the paper the OIA models are presented from a flow chart defining the variables and functions of the two models. Then, in the next paragraph, the Observation model, shared by the two methods, is detailed. In the fourth part, the two models are detailed. Finally, these two approaches are used to solve the multiobjective problem and are compared. To conclude, both methodologies are discussed and some perspectives are proposed.

2 Modeling Approach

2.1 OIA Modeling Approach. The OIA method aims at modeling design problems and translates them into global mono-objective optimization functions. Optimizations results computed from this function are design solutions related to optimal performances and global preference. The model of the design problem combines design objectives, design constraints and, eventually, designer preferences into a single objective of preference maximization. The modeling approach is divided in three steps illustrated in Fig. 1. Inlets (design variables denoted X) and outlets (preference variable denoted u) of the model are connected using an optimization objective function, which is

$$\text{Find } X^* \in \mathrm{D}_X\text{: max.u}(X), \quad \text{with} \quad u = \xi \circ \delta \circ \mu(X) \qquad (1)$$

where

$$X = [x_1, ..., x_i, ..., x_n]^T$$

Design variables (also called decision variables in the context of optimization theories) correspond to the system physical characteristics sought by designers to define a design solution. In the following these variables correspond to locations of holes along turbine blades or to the shapes of these blades, for instance. From design variables:

- the observation function (denoted μ) computes the physical behavior of the system being designed and assess physical observation variables (denoted Y)
- the interpretations function (denoted δ) translates each observation variable into interpretation variables (denoted Z)
- the aggregation function (denoted ξ) aggregates interpretation variables into the preference u

with

$$Y = [y_1, ..., y_i, ..., y_n]^T \quad Z = [z_1, ..., z_i, ..., z_n]^T$$

The optimization function selects each value $\mathrm{x_i}$ of X inside a domain of admissible values ranging between x_i^- and x_i^+. It is noticeable that in the following, we only consider discrete domains of values:

$$D_{xi} = \{x_i^-; x_i^+\}$$

The design search space is therefore the union of these sets

$$D_X = \bigcup_{i=1}^{n} D_{xi}$$

2.2 Objective Function. From the general framework presented above, two different objective functions are presented in this paper. The OIA methodology is originally oriented toward the combination of subjective and objective knowledge in design processes. However, in the context of complex industrial environments, designers may be reluctant to combine such types of knowledge inside a single model and, more to the point, the cost and delays of knowledge formalization are high since, at this stage, most of the subjective knowledge remains informal. Consequently, we propose two different models of the design problem which are presented in Table 1.

The first model takes account exclusively of physical or economical values and is oriented toward purely objective knowledge modeling. On the contrary, Z and u in the second model are defined on design scales [8] ranging between 0 and 1 and corresponding to desirability values. Both models turn the multiobjective optimization problem into a mono-objective one using the OIA modeling framework. However model 1 results in the ownership cost of the turbo-engine that must be minimized, whereas model 2 results in a global desirability (equivalent to a satisfaction) level that must be maximized.

Table 1 OIA models 1 and 2

Model	X design variables	Y observation variables	Z interpretation variables	u mono-objective variable	Goal
n°1	Activation of 14 air impingements Leakage thickness Leakage position Film cooling activation	Service lifetime Engine output power Engine specific fuel consumption	Fuel cost Payload cost Maintenance costs	Ownership cost	Minimization
n°2			Harrington's desirability functions: -Service lifetime -Output power -Fuel consumption	Derringer's aggregation function	Maximization
	$Y = \mu(X)$	$Z = \delta(Y)$	$u = \xi(Z)$		

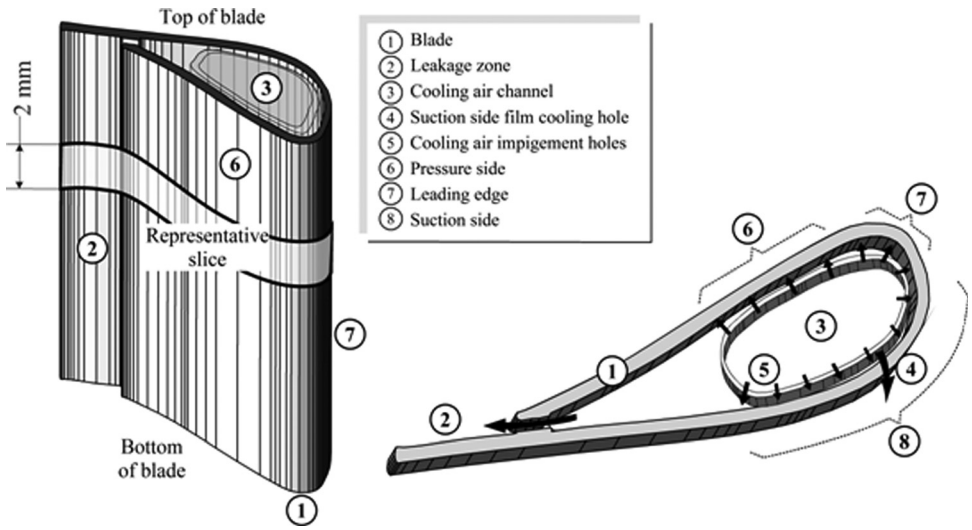

Fig. 2 Blade and representative slice

3 Design Variables and Observation Model

3.1 Design Variables and Their Corresponding Domains. In this paper, the blades of the first turbine stage NGV correspond to a medium power turboshaft engine of about 1000 horse power during take-off. Blades can be cooled with high pressure unburned secondary flow of air by means of impingement holes. Downstream of the blades, the cooling mass flow joins the main high temperature gas flow on the pressure side, close to the trailing edge or on the suction side, not far from the leading edge. Pressure in these locations is lower than the pressure inside the cooling system, which avoids aerodynamic losses and produces film cooling protecting the vane. It is noticeable that, in this study, we do not use devices such as ribs or pedestals used to enhance forced convection. The cooling air flow is transported inside the blade using an insert part going through the blade.

A first set of design variables is related to the activation of the impingement holes along the chord of the blades. As shown is Figs. 2 and 14 impingement rows can be activated: 7 on the suction side of the vane, 4 on the pressure side, and 3 at the leading edge. Two other design variables are related to the shapes of the blades. As shown in Fig. 3 (leakage position 1), using a long film cooling length and a narrow leakage area leads to a very thin trailing edge. On the contrary, short film cooling protections (Fig. 3, leakage position 3) or larger exits (Fig. 3, leakage thickness 2) increase the value of dihedral angle.

In the following, the domains of the values of the corresponding design variables are voluntarily limited and made interdependent to limit the complexity of the optimization process. Therefore, only one suction side film cooling row can be activated; using different locations for the impingements along the vane chord or leakage areas make the optimization difficult and tremendously increase the computational times. Pressure side mass flow can be ejected at 3 different locations with two different areas.

The domains of values of the design variables are defined in Table 2.

3.2 Observation Model. The observation model consists in thermal and aerodynamic efficiency models of the system. This

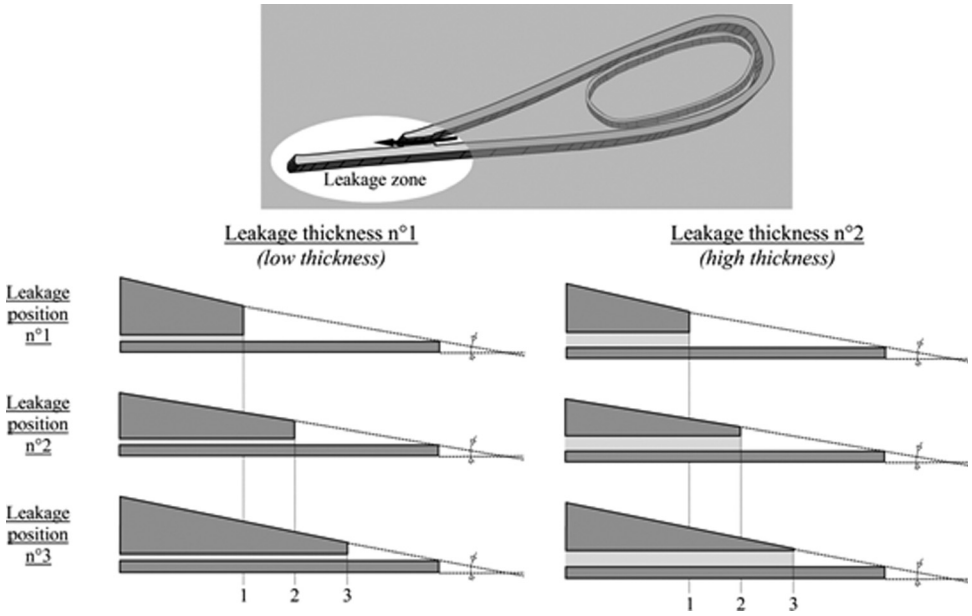

Fig. 3 Design variables related to the trailing edge of the blades

Table 2 Design variable domains

Design variable	Design variable domain	Meaning
x_1	$\{0;1\}$	Air impingement n°1 activation
⋮	⋮	⋮
x_{14}	$\{0;1\}$	Air impingement n°14 activation
x_{15}	$\{1;2;3\}$	Leakage position
x_{16}	$\{1;2\}$	Leakage thickness
x_{17}	$\{0;1\}$	Film cooling activation

model computes the lifetime of the blade and therefore of the NGV, engine specific fuel consumption and output power variations.

Figure 4 sums up the observation model, which is divided in four elementary models:

- the inner CFD model of the fluid inside the blade and the material of the blade, which computes the thermal efficiency of the NGV
- the service lifetime model, which computes lifetimes from the thermal behaviors of the blades
- the outer CFD model, which computes the efficiency enhancement or degradation of the turbine stage due to the blade cooling system
- the engine performance model, which transforms the previous efficiency variations into engine specific consumption and output power

3.2.1 Inner CFD Model. The inner CFD model is used to simulate the thermophysical phenomena occurring in the inner fluid between the inside face of the blade and the outside of the cooling air channel and inside the material of the blade. Three dimensional thermal simulations are performed by means of the computational fluid dynamics software ANSYS FLUENT®. The whole internal cooling system of one NGV blade is meshed and solved from the steady Reynolds-averaged Navier–Stokes (RANS) model. Fig. 5 shows the mesh used for the simulations.

NGV blades from their bottom to their top can be divided in slices since the air impingement holes are regularly spaced along the height of the blade. To simplify the physical model and decrease numerical computation times, the model only considers one representative slice of blade (periodicity hypothesis), the height of which is 2 millimeters. However, since the air flow surrounding the external surface of the blades differs along the height of the blades, this simplifying assumption is compensated by considering the slice for which the main burned gases RTDF effect is maximum. It is also noticeable that this hypothesis assumes that radial conduction within the blades does not affect simulation results. More to the points, in practice, designers may prefer irregular arrangements of impingement holes to compensate the irregular distribution of the thermal and mechanical constraints inside the blades. In such configuration, the periodicity hypothesis may be irrelevant.

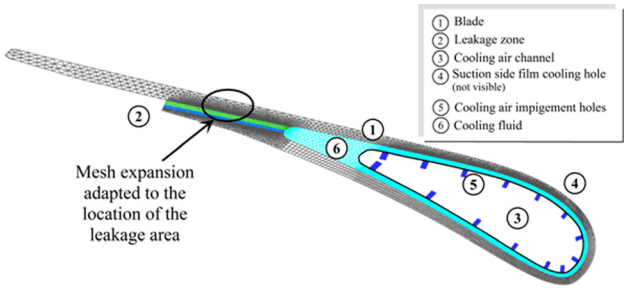

Fig. 5 Blade and inner fluid mesh

The model is made of about 1.3M elementary cells inside of the representative slice of blade. Most of the elements are tetrahedral but some prisms have been used to mesh the boundary layers, the fluid regions in the cooling holes and some zones of the metallic blade. Since, the mesh must be refined in particular zones of the representative slice according to the design of the blade, three similar meshes have been built to consider the different lengths of film cooling on the pressure side. At each stage of the optimization process one of these mesh is used according to the design configuration being simulated.

Boundary conditions (Fig. 6) are set from fixed pressures and temperatures or heat flux conditions. At the inlets of the impingement holes, the total pressures and temperatures are fixed to constant values corresponding to the supply pressures and temperatures of the cooling air channel. The walls of the impingement holes and the inner wall of the cooling flow hole are assumed to be adiabatic. In the same manner, the static pressures of the outlets of the leakage areas are fixed to the NGV outlet pressure. The inner walls of the vane are coupled with the cooling system. Finally, the thermal boundary conditions at the airfoil outer surface result from convection between the blade and the high temperature gas flowing through the NGV. Convection parameters result from simulations of the outer CFD model, which links inner and outer CFD models.

Heat transfer coefficients around the blades of the vane are computed by the outer CFD model. These coefficients are evaluated using the "in house boundary layer" program available in ANSYS FLUENT®. This program takes into account the intensity and pressure gradients of the turbulence at the outlet of the combustion chamber. The model carried out by this program is a k-ε turbulence model at low Reynolds numbers. Turbulence production and dissipation are corrected by the Lam–Bremhorst functions described by Schmidt and Patankar [9]. At the leading edge, a correlation derived from a publication of Sibulkin [10] is used to quantify the heat transfer coefficients near the forward

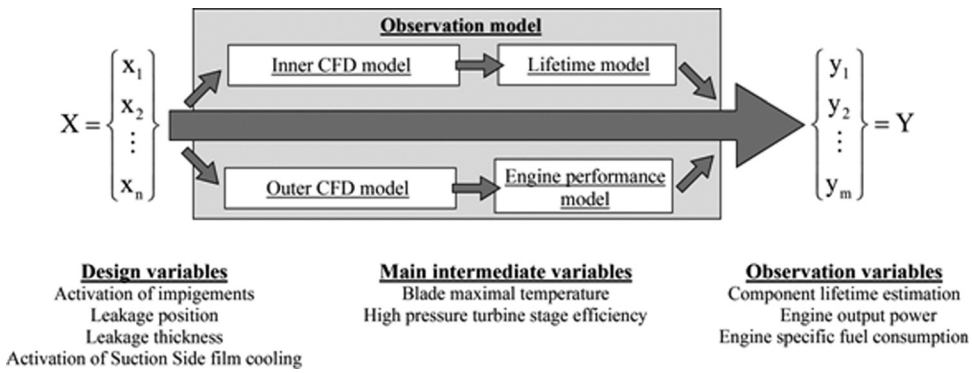

Fig. 4 Observation model flow chart

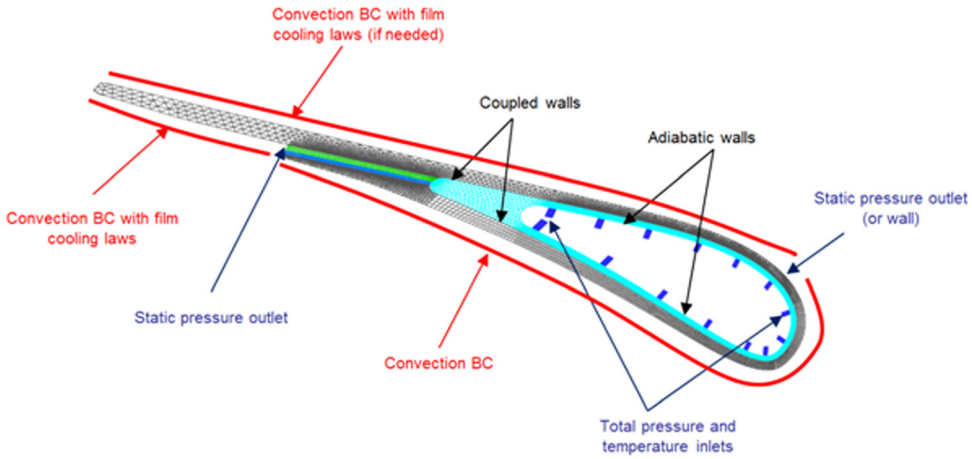

Fig. 6 CFD model boundary conditions

stagnation point of a body of revolution. The output values of the boundary layer program around the stagnation point are fitted according to this value.

Effectiveness laws of the "in house" film cooling are used to correct these convection inputs on the pressure side (*PS*) trailing edge wall and, if necessary, on the suction side (*SS*) surface. These correlations have the following form:

$$\eta_{\text{film\_SS}} = \frac{c_1 \cdot e^{c_2/\text{Re}^2}}{c_3 + c_4 \cdot e^{c_5 \cdot M^{c_6}} \cdot \left(\frac{s}{BL^2}\right)^{c_7}} \tag{2}$$

$$\eta_{\text{film\_PS}} = \frac{c_8}{1 + \left(c_9 \cdot \frac{s}{BL^2}\right)^{c_{10}}} \tag{3}$$

The topology modifications of the mesh required by the suction side film cooling activation, pressure side leakage area evolutions or closures of impingement holes are handled by design parameters. The meshing process is automatic and adapts the locations and dimensions of the fluid/solid zones and the number of nodes inside these different zones. As a result, pressure inlets or outlets are turned into walls if required.

It is noticeable that, due to couplings between physical phenomena, several loops of CFD simulations are required to solve each design configuration. The first loop is performed by computing the film cooling blowing ratios and, from their values, by updating the convection parameters. New film cooling efficiencies are then input and the mean temperature around the vane is updated to balance the enthalpy going through the turbine according to the following equation:

$$T_{40} = \frac{(\dot{m} \cdot Cp \cdot T)_{41} - (\dot{m} \cdot Cp \cdot T)_{\text{coolant\_PS}} - (\dot{m} \cdot Cp \cdot T)_{\text{coolant\_SS}}}{(\dot{m}_{41} - \dot{m}_{\text{coolant\_PS}} - \dot{m}_{\text{coolant\_SS}}) \cdot Cp_{40}} \tag{4}$$

Assuming a constant radial temperature distribution factor, the vane outer wall convection temperature is

$$T_{\text{convection}} = (T_{40} + \Delta T_{\text{RTDF}}) - \eta_{\text{film}} \cdot (T_{40} + \Delta T_{\text{RTDF}} - T_{\text{ejection\_film}}) \tag{5}$$

About 500 simulation tests have been performed on different candidate design solutions and the result analyses show that the convergence is always reached after three calculation loops. In the following, the optimization results are derived from these 500 tests.

Figure 7 shows the steps performed to solve the CFD simulation problem.

It also must be noticed that the model of fluid turbulence used in our approach is a low Reynolds mesh and k-w SST turbulence model, as recommended by Xing et al. [11]. However, Xing's recommendation limits the sizes of mesh elements from a nondimensional value of wall distance denoted y^+, which must not exceed the value of 2 according to these authors. This tends to increase computation times of simulation and several coarser meshes have been tested to analyze the sensitivity of the size of element. From this analysis, it has been proved that the size of element has low influence on such simulation results, in particular in the most critical parts of the blade such as the trailing edge. This mainly results from the local temperature of the gas mainly driven by film cooling efficiency laws and combustion chamber exit temperature (computed from the coolant mass flow). In our model, the nondimensional wall distance ranges between high values of 20 to 75 and values of 2 as recommended by Xing et al.

3.2.2 Lifetime Estimation. The maximal metal temperature of the blade is derived from the previous fluid dynamics computations and this temperature is related to the maximum admissible number of cycles for the engine (engine start and shut down). This model is a function relating the number of cycles of the NGV to the highest temperature of the blades. It has been developed from experimental measurements of temperatures and endurance tests performed on NGVs. The minimal number of cycles of the vane is limited to 100 in this function. This function is presented in Fig. 8. However, for confidentiality reasons, temperature values on the figure are nondimensional and related to the gas temperature at the outlet of the vane. This gas temperature remains higher than the metal temperature of the blades and; consequently, the nondimensional values are lower than 1.

From the maximum admissible number of cycles of the NGV and from the average mission durations defined in the design

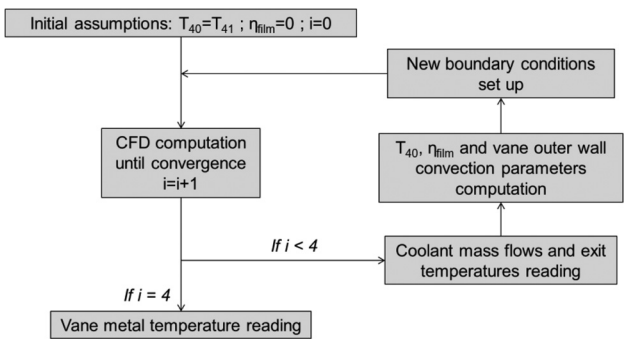

Fig. 7 Aerothermal problem solving diagram

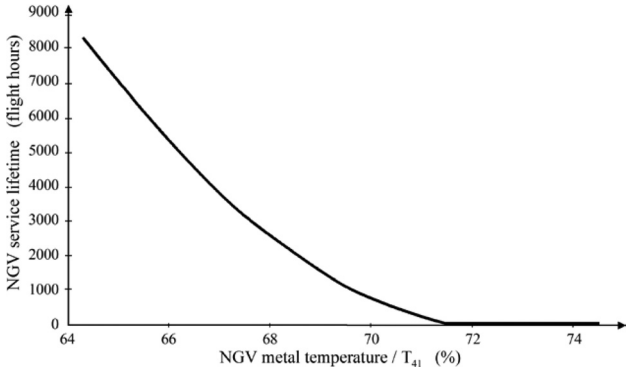

Fig. 8 NGV life evolution with maximum metal temperature

requirement documents, the metal temperature of the vane is converted into expected lifetimes.

3.2.3 Outer CFD Model. Aerodynamic performances of blades are computed from two specific mechanisms of energy degradation models hereafter called models of losses and corresponding to profile/trailing edge losses and suction side film cooling losses.

As discussed in Ref. [12] and illustrated in Fig. 9, pressure and velocities around the trailing edge of a blade depends on the trailing edge shape and thickness. To increase the pressure side film cooling effect with a reduced film cooling length (leakage position n°3) or to blow more cooling mass flow with a thicker leakage film, the dihedral angle at the end of the vane must be high.

The profile/trailing edge losses have been estimated by means of specific 3D aerothermal transonic computations performed for three different vane shapes. These three different shapes correspond to one short, one large and one intermediate trailing edge and range between the extreme values considered in the following computations. To obtain accurate values, the whole turbine stage was taken into account in this model, including vane end-walls, the rotor blade and its casing. An adiabatic low Reynolds RANS model was used from the ONERA ELSA software [13]. From these simulations, a linear correlation linking dihedral angles with turbine stage efficiencies has been derived and is used to quantify the aerodynamic properties of the air flow surrounding the blades. These three CFD computations have also been used to compute the static pressure variations in the leakage zone.

$$\Delta\eta_{\text{trail}} = b_1 \cdot \alpha \tag{6}$$

The correlation combined with film cooling effectiveness functions result in a model the solving of which requires low computation times. The main computational efforts are linked to the simulation of the internal cooling system and metallic blade temperatures. Meshing the main gas flow would have led to unacceptable computational costs in regard with the optimization process carried out in this paper.

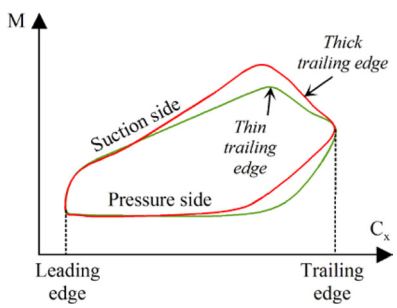

Fig. 9 Impact of dihedral angle on Mach numbers

As proposed by Ireland [5], the suction side film cooling loss is quantified by means of Hartsel's expression [14]. This equation estimates the pressure loss due to mixing film cooling air with the mainstream gas. This loss is driven by the mass flow characteristics at the suction side outlet computed by the CFD model. In this equation, it is further assumed that η_{SS} equals one, which; in other words means that the pressure side film cooling losses are supposed to be low compared with the efficiency value; this hypothesis has been verified and accepted from preliminary analyses, mainly because of the similarity of the Mach numbers of the gas flows of coolant gas and burned air.

$$\Delta\eta_{SS} = 2 \cdot \left(\frac{Mn_{\text{coolant}}}{Mn_{\text{main\_flow}}}\right)^2 \cdot \dot{m}_{\text{coolant}} \cdot \left[1 + \frac{T_{\text{coolant}}}{T_{\text{main\_flow}}} - 2 \cdot \frac{V_{\text{coolant}}}{V_{\text{main\_flow}}} \cdot \cos\alpha\right] \cdot \eta_{SS} \tag{7}$$

3.2.4 Engine Performances. The design of the nozzle guide vane acts on the engine performances through the high pressure turbine. The efficiency of this turbine is influenced by the energy degradation phenomena occurring inside the NGV since these energy degradations are irreversible and cannot be recovered.

Dealing with efficiency drops of high pressure turbine at early design stage can be performed by:

- increasing turbine entry temperature: in this case, the engine power is preserved but the fuel consumption rises and the service lifetimes of the components downstream of the hot section are lowered
- increasing the area of the low pressure nozzle: the mechanical load of the high pressure blade is higher and the output power decreases as the loading of the low pressure turbine decreases, this would have an influence mainly on fuel consumption.
- letting the engine find its new operating conditions: both fuel consumption and output power are transformed as the engine overhaul pressure ratio is reduced

In the following, we limit our investigations to the last option and the balance of heat and mechanical loads of the turbine stages is preserved in the model. Variations of engine specific fuel consumption (ΔSFC) and output power variations (ΔPW) are expressed by means correlations according models of losses. Correlation coefficients are obtained by experiments realized on similar turboshaft engines.

$$\Delta\text{SFC} = b_2 \cdot (\Delta\eta_{\text{trail}} + \Delta\eta_{SS}) \tag{8}$$

$$\Delta\text{PW} = b_3 \cdot (\Delta\eta_{\text{trail}} + \Delta\eta_{SS}) \tag{9}$$

4 Objective Functions

4.1 First Model of Objective Function. The first model of objective function proposed in this paper is based on the transformation of observation variables into passenger costs per flying hour (interpretation) and the addition of these costs into a global cost indicator (aggregation). In particular, we use functions derived from data proposed by Sallee [15]. Those functions compute fuel costs and direct maintenance costs from levels of deterioration of jet engines.

The general structure of the model of the objective function is presented on Fig. 10. This model transforms the observation variables into fuel, payload and overhaul costs per flight hour. Cost aggregation is obtained by summing these three costs to obtain a global cost indicator to be minimized.

4.1.1 Interpretation Model Model: Fuel Costs. Excluding take-off and idle periods, the engine hourly amount of fuel consumed *FB* can be computed from the specific fuel consumption, Power of the engine and fuel density as

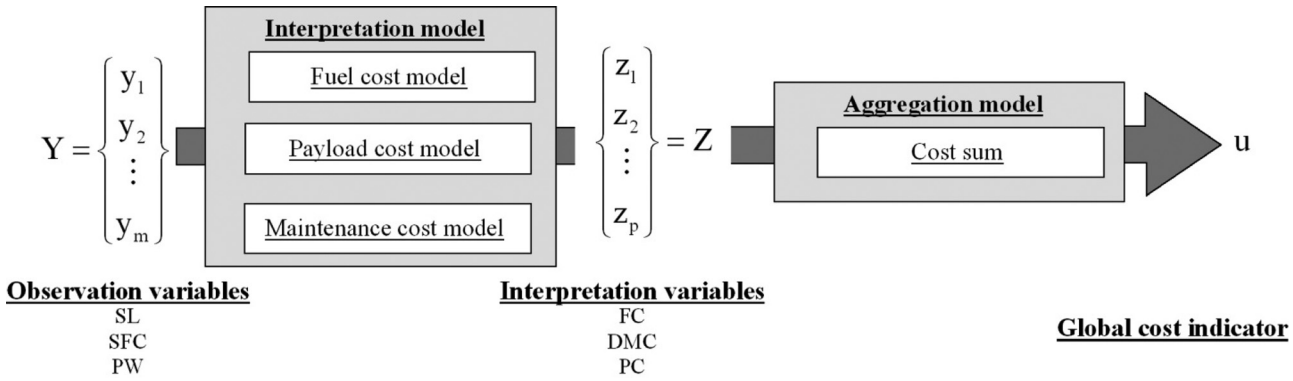

Fig. 10 Objective function of the first model

$$FB_{cruise} = \frac{PW_{cruise} \cdot (SFC_{cruise} + \Delta SFC_{cruise})}{\rho_{fuel}} \tag{10}$$

Due to oil prices fluctuations, calculating the cost corresponding to this consumption is more hazardous. To compute and estimate fuel consumption costs FC, we use the EIA forecast [16] database and the low sulfur crude oil price growth from today to 2030. FC is computed with

$$FC_{cruise} = FB_{cruise} \times JFP \times \frac{oil_{2030}}{oil_{2010}} \tag{11}$$

Fuel consumption also influences the payload of the tank of the aircraft but the size of the tank is also highly dependent of the length of the long range missions of the aircraft.

4.1.2 Interpretation Model: Payload Costs. Environmental conditions have a major impact on the engine performances. Consequently, engines are generally oversized by taking into account the worst international standard atmosphere conditions at ground level. As a result, helicopter payloads vary with engine power only in tropical operating conditions. As an example, constructor data [17] shows that Sikorsky S76C++ aircraft maximum transmission torque limit is reached if ambient condition reaches 30 °C at low altitude. In this study, the authors assumed that studied engine is designed to perform oil off-shore taxi missions. Based on current offshore rig distribution by region [18] and climatic data, estimated percentage of customers running their aircraft limited by engine performance can be computed. Considering a rig in these conditions if at least one monthly average temperature is excess of 29 °C, 59% of rigs are limited by the engine power.

The helicopter maximum permissible take off weight in tropical conditions (MPTOW) is estimated from data of take-off power and aircraft maximum takeoff weight. This value is then related to the aircraft payload, itself linked to the blade characteristics through the global model. Given the average total variable cost TVC relative to a medium two engine aircraft [19].

Finally, from payload change due to engine output power deterioration, payload fare can be computed, as shown in the following equation:

$$PC = \frac{tropical\_rig}{total\_rig} \cdot \frac{TVC}{MPTOW - fuel - OEM} \cdot \left(\frac{\Delta PW_{take\_off}}{PW_{take\_off\_initial}} \cdot MPTOW \right) \tag{12}$$

To conclude, as an example, considering a Sikorsky S76C++ aircraft for this study, for every 1% turbine stage efficiency decrease, customers would experience an average of € per flight hour cost increase due to payload drop.

4.1.3 Interpretation Model: Maintenance Costs. Through their life cycle, engine parts such as NGV are repaired or overhauled and the cost of their maintenance is high with regard to the ownership cost of the whole engine. Direct maintenance costs (DMC) must be taken into account early in the design process since these costs highly influence the economical performances of the system and; consequently, the life cycle of turbo-engines. NGV is one of the most critical parts of these engines since this vane are submitted to very high temperatures degrading their performances through time.

In the following, we use a function of DMC (see Fig. 11) related the ratio between the maximal metal temperature of the NGV and the temperature T_{41} (at the outlet of the NGV) to the DMC of the whole engine. Again, we use such nondimensional temperature definition and the values of costs remain undefined on the figure for confidentiality reasons. This function has been built from experiment and, more precisely, from database of engine dismantling operations, part manufacturing and engine renting during maintenance operation; these database are therefore based on internal prices of the TURBOMECA society and have been extrapolated using a constant profit margin to transform them into DMC values.

From Fig. 11, it can be noticed that DMC tend to very high values as soon as nondimensional temperature values reach the threshold of 0.71. On the contrary, NGV metal temperature has a quasi-negligible influence on the engine direct maintenance cost if this value is inferior to 0.665.

4.1.4 Aggregation Model. The aggregation model consists in making a global indicator from the values resulting from the interpretation model. As these interpreted values are costs, they can be added to build a global indicator cost, which must be minimized

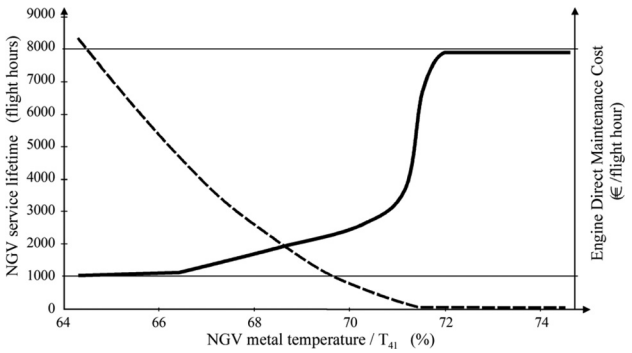

Fig. 11 Direct maintenance cost

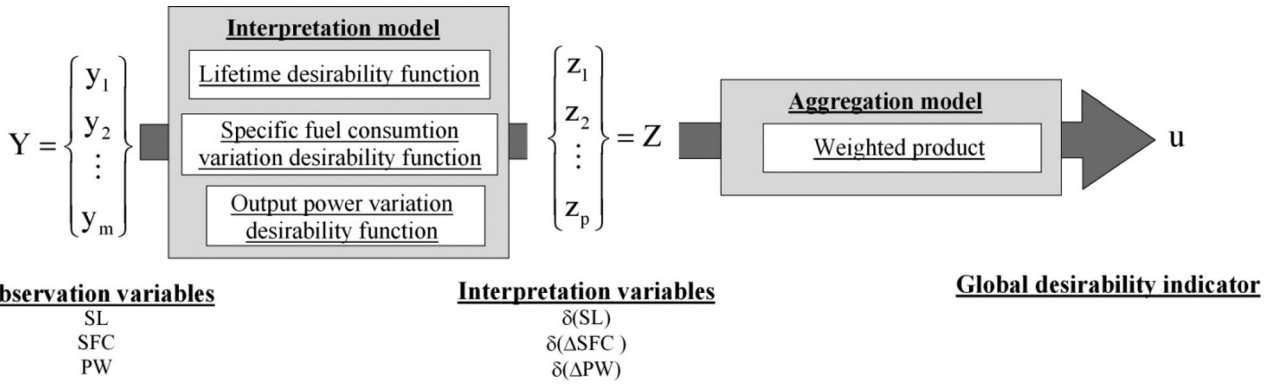

Fig. 12 Objective function of the second model

through the optimization process. This indicator is an ownership cost related to the customer of the engines; customers will pay for fuel, payload and maintenance. From the point of view of the designer and manufacturer of the engine, minimizing this cost results in improving its own capability to optimize the compromise between profit margin and customer's satisfaction, which itself also depends on the competitive environment of the engine.

Fuel and maintenance costs are proportional to the number of engines (N_e) and the global cost indicator can be expressed as

$$u = N_e \times FC + N_e \times DMC + PC \tag{13}$$

In the following application, we consider a twin engine aircraft and; consequently, we use

$$N_e = 2 \tag{14}$$

Such an approach of multicriteria aggregation consists in relating every observation variable to one cost value, costs having the particularity to be conservative (since manufacturer and customer cannot create or destroy money) and tangible economic quantities. They are additive values provided that these monetary values are equivalent, which means that they are traded in strictly similar conditions. For instance, at any given moment, fuel and maintenance are paid on a regular basis by the customer according to the number of flight hours he has performed; FC and DMC therefore seem to be equivalent. However, fuel prices are fluctuant and less predictable than maintenance costs. Engine manufacturers and most of their customers are often involved in some sorts of partnerships, whereas fuel providers and customers are not. Customers can perceive risks underlying the cost of fuel as being much higher than maintenance costs, which is out of the scope of this first model of objective function. In a more general manner, additivity assumes that the uncertainties related to the models from which the costs are derived are low. Optimizing the global indicator u defined by Eq. (10) might therefore lead to unrealistic design solutions.

Another approach is based on the direct formalization of designers' objectives through desirability functions. This approach aims at avoiding the constraints of cost based interpretation and aggregation methods and has been developed in the domain of multicriteria decision analysis dedicated to engineering design.

4.2 Second Model of Objective Function. Facing with complexity inherent to complex mechanical systems, designers' objectives are usually managed through design requirements documents, in which elementary technical objectives are fixed during the preliminary phases of the design process. Design requirements are derived from a tool classically used in design departments and identified as design functional analysis. Through this tool, designers define every elementary objective of the design problem with criteria involving observation variables and their acceptable limits and flexible values. As an illustration, the energy efficiency of an engine could be related to a minimal admissible value, let's say 80%, and a tolerance threshold on this admissible value of 0.5%, which in this case means that a precision lower than 0.5% on the value of 80% is not relevant.

In regard to functional analysis based approaches, interpreting and aggregating all of the design objectives into a single global cost indicator is equivalent to transform the objectives into cost indicators from economical analysis. Such a transformation first demands supplementary efforts to designers' teams and next often leads to doubtful models since the economical analysis generally relies on numerous simplifying hypotheses. Turbo-engines design objectives should, in this case, rely on the complete analysis of helicopter markets and their human or physical environments. Desirability based approaches aim to directly interpret the design satisfaction criteria derived from functional analysis on the same design scale. Interpretation and aggregation are performed on a scale of desirability, namely a scale of satisfaction of designers. Satisfaction is interpreted on a 0 to 1 scale and, from this scale designers can model and take into account through simulation or optimization processes objective or more subjective knowledge.

Figure 12 presents the general structure of the model based on desirability functions. Interpretation consists in transforming the observation variables into desirability values and aggregation in computing a global desirability indicator from the weighted product of these elementary desirability values.

4.2.1 Interpretation Model. Harrington's desirability functions [20] are used in many different domains to formalize designer's satisfaction (see Fig. 13). Using those functions δ parameterized with two values AUC_i and LSL_i, every observation variable y_i is transformed into one or several desirability levels. Every function is related to one particular design criterion and translates design criteria into numerical functions. Values close to 1 correspond to highly desirable values of the corresponding observation variable and values close to 0 are highly undesirable.

Parameters AC and SL respectively correspond to the values of "accurate constraint" and "lower soft limit" of the function, namely to values beyond which desirability becomes insensitive to the value of the observation variable. In the case of turbo-engines, these values have been determined from designers' expertise. They are mainly based on return on experiments and comparisons with previous design projects or competitors' engines. Designers perceive the products they are designing as continuously evolving systems in a competitive environment. Expertise encompasses much information out the of the scope of the global cost indicator presented in the model 1 such as priority, risk, and so on; it is also noticeable that expertise is generally more tolerant to error than analytic models.

For confidentiality reasons the parameters of the specific fuel consumption variations and output power variation cannot be here

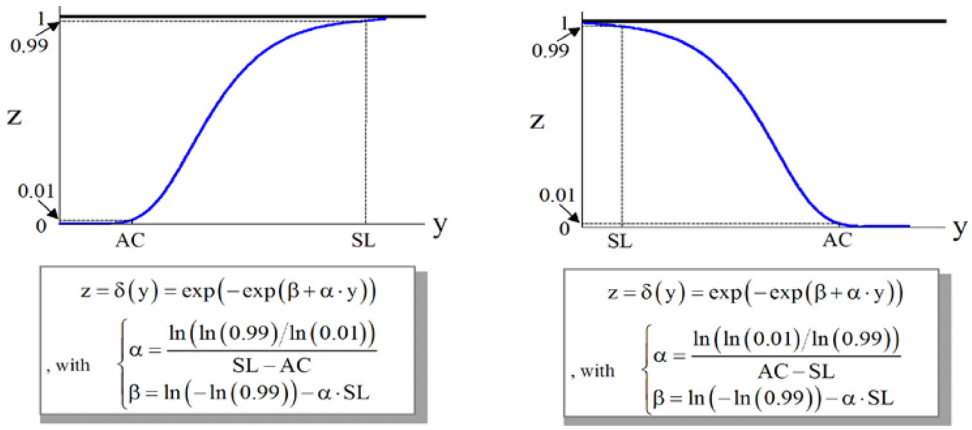

Fig. 13 Harrington's desirability functions

disclosed. However, the interpretation function of the service lifetime is presented on Fig. 14. This function has been settled from the values of 3000 and 6000 h, the first service lifetime being regarded as extremely low (desirability 1%) and the second as high (desirability 90%).

4.2.2 Aggregation Model. Interpretation variables Z are combined into a single variable u, which transforms the design problem into a mono-objective optimization problem. Since u is a global desirability indicator, it must be maximized. Several methods have been developed to aggregate variables [20] and develop global indicator values. In the following, we use a weighted product first proposed by Derringer [21]:

$$u = \xi(z_i, \omega_i) = \prod_{i=1}^{3} z_i^{\omega_i} = \prod_{i=1}^{3} \delta(y_i, AC_i, SL_i)^{\omega_i} \tag{15}$$

with,

$$\Omega = (\omega_1, \omega_2, \omega_3)^T \tag{16}$$

Aggregation functions dedicated to design have been investigated within the framework of multi-criteria decision analysis. In particular, Scott and Antonsson [22,23], and Messac [24] investigated several types of aggregation methods and classify these methods according to the concept of "design appropriate function."

Weighted product satisfies to every constraint of being "design appropriate" and, in particular, it satisfies to the property of annihilation. Design solutions are undesirable (u=0) if and only if one desirability value is nil; namely, a design solution is invalid as soon as it does not satisfy to at least one of the design criteria. More to the point, each of the weighting parameters ω_i corresponds to the relative level of priority allocated to one particular design criterion of which satisfaction is the value of z_i. High values of ω_i correspond to high levels of priority and; on the contrary, low values of ω_i correspond to low levels of priority. Weighted product aggregation functions are said to be compensatory, since priority may compensate desirability and vice and versa.

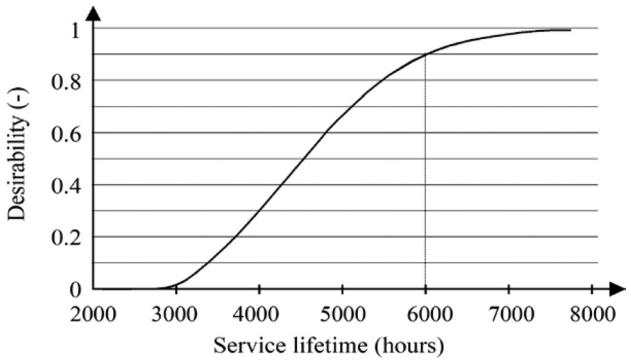

Fig. 14 Service lifetime desirability function

Weighting parameters for the NGV have been settled from interviews and using the method of the analytic hierarchy process (AHP) proposed by Saaty [25]. It consists in making pairwise comparisons between the levels of importance of the different criteria of the design problem. Knowing that every design criterion corresponds to an interpreted variable, this consists in weighting the level of significance of every component of Z and; therefore, to settle parameters ω_i. These parameters are derived from a judgment matrix, which is, squared, symmetrical and whose terms are defined on a scale ranging from 1/10 to 10. In this matrix, if A(i,j) = a and A(j,i) = 1/a and lines or rows "i" and "j" correspond to two criteria (n°1 and n°2), this means that the relative level of importance of criterion n°1 is "a" compared to criterion n°2. The higher is "a" the higher is the significance of criterion n°1. Knowing that the NGV design problem is related to three design criteria, matrix A is

$$\mathrm{A} = \begin{bmatrix} 1 & a_1 & a_2 \\ 1/a_1 & 1 & a_3 \\ 1/a_2 & 1/a_3 & 1 \end{bmatrix} \tag{17}$$

The mathematical implications of these levels of importance should be detailed but are out of the scope of this paper; they are detailed in Ref. [22]. According to the theory of Saaty, the weighting parameters are derived from the maximum eigenvalue λ_{max} and its corresponding eigenvector of the matrix A. This eigenvalue satisfies to

$$\lambda_{max} = 1 + d + d^{-1}, \quad \text{with:} \quad d = \left(\frac{a_1 \cdot a_3}{a_2}\right)^{1/3} \tag{18}$$

The weighting parameters ω_i are then derived from the principal eigenvector divided by the sum of its terms, and for a squared matrix of dimension 3

$$\Omega = \left(\frac{a_2 \cdot d}{1 + a_2 \cdot d + a_3/d}, \frac{a_3}{d \cdot (1 + a_2 \cdot d + a_3/d)}, \frac{1}{1 + a_2 \cdot d + a_3/d}\right)^T \tag{19}$$

Table 3 Judgment matrix

	δ_1(SLT)	δ_2(ΔSFC)	δ_3(ΔPW)
δ_1(SLT)	1	1/4	2
δ_2(ΔSFC)	4	1	3
δ_3(ΔPW)	1/2	1/3	1

Judgment matrices may contain contradictory values and be inconsistent. The weighting parameters derived from these matrices roughly correspond to average values of levels of importance defined in the matrices. Saaty introduced a consistency ratio to compute the levels of consistency of judgment matrices, which are regarded as consistent enough provided that this ratio is lower than 10%. For matrices of size 3, this consistency ratio is

$$RC = \frac{\lambda_{\max} - 3}{2 \cdot 0.58} \tag{20}$$

The judgment matrix of the NGV optimization problem has been settled from interviews of designers working at different decisional levels inside a design department. Therefore, these values reflect a consensus among designers which agree on the relative levels of importance of the three design criteria

$$\mathrm{A} = \begin{bmatrix} 1 & 1/4 & 2 \\ 4 & 1 & 3 \\ 1/2 & 1/3 & 1 \end{bmatrix} \tag{21}$$

Table 3 shows the interpretation of matrix A. The power variation (ΔPW) is regarded as the less important criterion compared to the two others. On the contrary, the specific fuel consumption (ΔSFC) is regarded as the most important. Using Saaty's scale ranging from 1/10 to 10 and its corresponding semantic scale, the values of 2, 3 and 4 correspond to "slightly more important" to "significantly more important" evaluation levels. These values are independent of the desirability values and must be interpreted as evaluations of the risks inherent to the failure of the criterion (criticity).

Specific fuel consumptions of turbo-engines are highly critical in aeronautic applications since fuel consumption influences the mass of embedded fuel and structural masses of aircrafts. Fuel consumption is the main item of expenditure of aircrafts and; consequently, even small gains of consumption are regarded as being of high importance. The service lifetime mainly influences the maintenance of the engine, which is also a major item of expenditure. In this context, the engine power is considered as being a secondary objective since losses of power may be compensated by a reduction of embedded load.

Matrix A leads to the following weighting parameters:

$$\Omega = (\,0.1515, \quad 0.6301, \quad 0.2184\,)^T \tag{22}$$

The consistency ratio of the matrix is lower than 10% and

$$RC = 9.2\%$$

Consequently, the global desirability indicator is

$$u = z_3^{0.1515} \cdot z_2^{0.6301} \cdot z_1^{0.2184} \tag{23}$$

5 Results and Discussion

5.1 Solution Set Analysis. Before performing the complete optimization process, tenths of simulations have been carried out to analyze the values of the observation variables. Among these solutions, one of them corresponds to a reference design solution (initial design), namely, a design solution first proposed by designers and developed independently from the optimization process using the normal procedure of decision within the design department of the company. Figure 15 shows the turbine stage efficiencies and NGV service lifetimes corresponding to these design solutions. The reference design solution is substantially less efficient and has a shorter service lifetime than several other solutions. Considering now every observation variable of the design problem, this solution has been proved to be non-Pareto optimal, namely, it performs less than some other solutions when considering every observation variable. Such a performance improvement tends to validate the optimization process proposed in this paper but must be completed from experimental investigations.

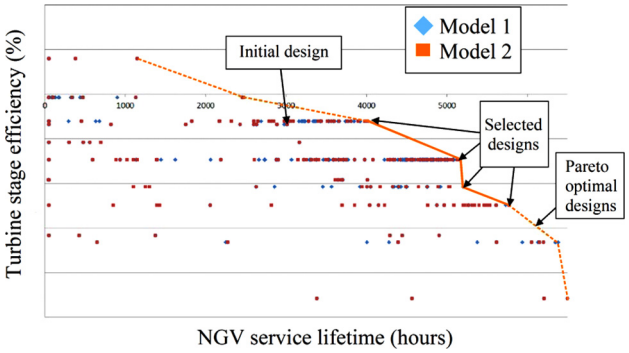

Fig. 15 Design exploration results

Candidate solutions on the left of the figure correspond to solutions with low lifetime capabilities but high aerodynamic performances. On the contrary, candidate solutions on the right are related to high service lifetimes but low aerodynamic performances. The Pareto optimal design solutions (relative to the two variables of the figure) correspond to values better than any other solutions according to at least one of the two design criteria. Pareto optimal solutions delimit a broken line called Pareto frontier, which is decreasing and shows that improving turbine stage efficiencies is detrimental to the service lifetime of the NGV. Improving turbine efficiencies tends to increase gas temperatures, which in turn tends to decrease the service lifetime of the NGV.

Figure 15 also shows that, whereas service lifetimes match many different values, turbine stage efficiencies are distributed according to only 12 different values making rows of points on the figure. These rows correspond to the combinations of blade shapes resulting from 6 different dihedral angles (3 leakage positions and 2 leakage thicknesses) and film cooling on the suction side (activated or not). Turbine stage efficiencies are therefore determined from gas cooling of the blades in the leakage zone or suction side. Increasing cooling limits the temperature of the blades, which improves their service lifetime, but decreases gas temperatures, which is detrimental to turbine efficiencies.

Finally, it should be noticed that, due to the simulation cost of design candidate solutions limiting the number of simulations, the solutions presented on Fig. 15 result from a snapshot of the population of solutions obtained during an optimization process. Consequently, these solutions have been generated through a convergent process avoiding most of the undesirable solutions. Such a population is not strictly representative of the performances of the complete set of solutions candidate to the design problem.

5.2 Optimization. Optimization is performed using an adaptative evolution algorithm [26] available in the software NEOSIS OPTIMUS®. It is based on the simulation of a simplified biological system evolving in a competitive environment. Candidate design solutions are defined from vector X and submitted to a selection process with mutations and crossing operators. Several candidate solutions are competing among a population made of 85 individuals through an iterative process. Every candidate solution

Table 4 Optimal design description

	Impingement cooling leading edge	Impingement suction side	Impingement pressure side	Leakage position	Leakage thickness	Film cooling activation
Reference solution	111	0101010	1110	3	1	0
Optimal solution	111	0110011	1111	2	0	1

is characterized by a set of values selected in the domain D_X and is evaluated from one simulation resulting in the value of u.

Each iteration of the population is called a generation. The results presented in the following are computed from 30 generations and the population is made of 85 individuals. At the end of each iteration, the five best candidate solutions of the population are selected to make the next generation using the mutation and crossing operators. More to the point, it is noticeable that the optimization processes corresponding to the two models of objective functions have been carried out independently.

Both of the optimization processes performed using the two models of objective functions converge toward the same solution. This solution is presented in Table 4. This solution is also displayed on Fig. 15. It corresponds to the optimal compromise between the 3 design objectives related in both cases (objective functions 1 and 2) to the 3 interpretation variables. It corresponds to a design solution characterized by:

- the index value of the thinner leakage (index 0)
- the intermediate film cooling position (index 2)
- the film cooling protection on the suction side of the blade is activated
- most of the impingement cooling rows activated

Figure 16 shows the fields of temperature of the reference and optimal design solutions. Temperatures on the figure are nondimensional and relative to the maximal temperature of the blades. The figure highlights that the maximal temperatures are attained in the case of the reference solution, which is detrimental to the service lifetime of the blade. Maximal temperatures are reached in the trailing edge of the blade because of the length of this edge, in the leading edge and suction side of the blade because of the nonactivation of the film cooling and upstream to the leakage zone because of the relatively high number of the closed impingement holes.

5.3 Discussion

5.3.1 Comparison Between Optimized Solution and Reference Solution. The NGV solution derived from the optimization process, whatever the objective function is, corresponds to a design solution more reliable than the reference solution, which tends to decrease the maintenance cost of the engine. Maintenance cost is lowered by decreasing the temperature of the material of the blade, however, this requires some dilution of the gas on the external surface of the blade using cooling air flows inside and outside of the blade. These flows are detrimental to the performances of the engine since their action is antagonist to the transformation of kinetic energy and pressure of the gas into mechanical energy. Gas dilution decreases its temperature and therefore the exergy available in the gas for the transformation. As an illustration, we compute that this increases the cost of engine flight per hour of some Euros and decreases the available payload of 30kg. Despite this degradation of the engine performances, maintenance costs are high enough to make engine reliability preferable to exergy transformation.

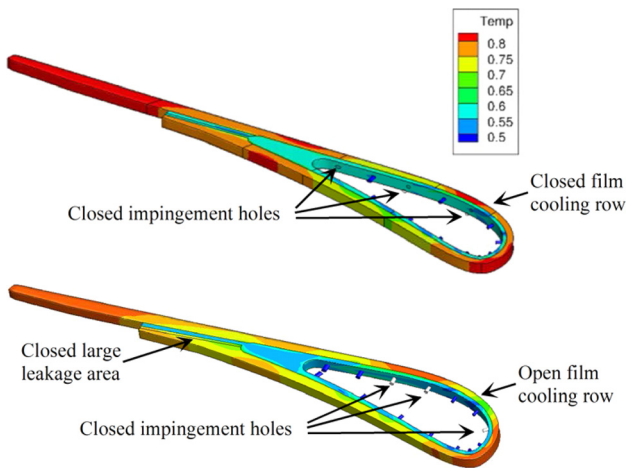

Fig. 16 Reference (on top) and optimal solution (on bottom)

Film cooling performed on the suction side of the blade has a major influence on the objective function value. Film cooling blows out the cooling mass flow on the suction side of the blade, which limits the cross-flow and decreases the thermal efficiency of the impingement jets located downstream of the suction side. Since less mass flow is available to decrease the temperature of the blade, temperature in the cooling system increases and the film cooling protection on the pressure side is less efficient.

Since some part of the mass flow is blown out of the blade on the suction side, the leakage section is low since cooling the blade requires less air. Consequently, the trailing edge is thin and the length of the pressure side film cooling protection is short. More to the point, since film cooling protection on the suction side is low, vane cooling must be performed by increasing the dihedral angle; however, this increases aerodynamics losses of the profile and; thus, energy degradation.

Finally, it must be noticed that the coolant mass flow of the optimized solution is lower than the one of the reference solution. This tends to lower the enthalpy consumption at the inlet of the turbine but increases energy degradation. Enthalpy consumption lowering does not offset energy degradation, but it increases service lifetime of the vane significantly.

5.3.2 Balancing Maintenance and Operative Costs. The cost objective function is minimized by designing Nozzle Guide Vanes for which service lifetimes and aerodynamic performances are close to the ones of the other components in the hot section of the engine. Designing vanes whose service lifetime is excessive negatively impacts on the engine cost. Reducing the engine time between overhaul significantly decreases the engine cost, but reducing the maintenance costs leads to more significant cost reductions. By balancing the aerodynamic losses and cooling method, designers can significantly reduce engine operative costs. Saving some euros per flight hour decreases the total engine operating cost of about 1%.

5.3.3 Robustness. Optimality of solution regarding objective functions is not sufficient to convince decision makers in design departments. The robustness of the method leading to the solution and the robustness of the solution submitted to stress tests are also important.

Concerning the robustness of the method used to formulate objective functions, it clearly appears that the method based on desirability functions (model n°2) is much more robust than the method based on cost modeling (model n°1). Model n°2 results from a direct mathematical formulation of data expressed in the design requirement documents of a turbo-engine. The

development of model n°1 necessitated the collection and interpretation of new data out of the scope of design procedures carried out in the design department. In other words, desirability based modeling of design objectives requires much less efforts than cost based modeling and, in this context, seems less risky. Collecting and gathering cost models data has been experienced as a challenge: it involves many people from different fields and deals with complex information. Before running the optimization process and discovering that both approaches lead to the same solution, designers were much more confident in cost based methods, despite the numerous and restrictive hypotheses taken into account through their development. Desirability based models are perceived as being subjective whereas they are based on reliable information tested through many different projects. From a practical point of view, it has been estimated that the development time of model n°2 was four times lower than the development time of model n°1.

Concerning the robustness of the design solution itself, stress tests have been performed to estimate the reliability of the solution. The first tests consist in testing the optimality of the solution by using new crude oil projection scenarios proposed by Newell [16]. The high and low scenarios of fuel prices have been taken into consideration and, despite the high variations of jet fuel prices, the optimal solution remained optimal. This is due to the fact that, since the domains of values of the design variables are discrete, the close neighborhood of every design solution is empty and the optimization process must jump from one solution to another. A design solution may remain optimal despite the perturbation of the parameters of the model.

Another stress test consisted in proposing a new judgment matrix and; consequently, a new set of weighting parameters ω_I for the aggregation model. This new judgment matrix resulted from new interviews of the actors of the design department. The new aggregation model significantly lowered the weighting parameter related to the fuel consumption and the initial optimal solution remained optimal despite this transformation of the optimization objective function. Finally, the stress tests highlight that the discretization of the domains of values of the design variables is too much coarse to make the optimal design solution sensitive to perturbations of the objective function. Further investigations proved that using six values of the leakage position for the film cooling in spite of three leads to significant turbine efficiency improvements.

6 Conclusion

In this paper, a design method based on physical behavior and global preference modeling and on numerical optimization has been applied to the design of the nozzle guide vanes of turboshaft engines. It has been carried out in the framework of the design department of a major engine manufacturer. The physical behavior model is a complex 3D aerothermal model taking into account several cooling alternatives of the turbine airfoils. These cooling systems aim to improve the service lifetime of the nozzle guide vanes. The design alternatives (design variables) concern the activations and positions of the cooling impingements and leakage section of blades. Optimization results in the best cooling alternative for the blades by taking into account multiple design objectives.

Preference modeling consists in developing an optimization objective function, which takes into account several design objectives. Two optimization objective functions have been developed and compared. The first one is based on the modeling of a global cost indicator; every design objective is related to one particular cost and the costs are added to obtain the global cost indicator. The second objective function results in a global desirability indicator. Every desirability function translates one design objective defined from design functional analysis (in design requirement documents) into satisfaction levels. The desirability functions are then aggregated into a single indicator using a judgment matrix (analytical hierarchy process). The judgment matrix defines priority levels between the design objectives. It has been determined from interviews performed in the design department.

Preference modeling based on costs is regarded as being objective, whereas the one based on desirability is regarded as being subjective by the actors of the design department. However, both approaches lead to the same optimal solution. More to the point, the overall development time of the first model was about four times higher than the second one. The desirability based approach mainly translates design requirements classically used by designers into mathematical formulae, which limits the development time of the model. Moreover, preference based on cost modeling requires various hypotheses affecting the objective character of the preference model. These factors would suggest that preference models based on the aggregation of desirability functions are more suitable for design optimization than preference models based on the addition of costs. However, a more advanced analysis (robustness analysis) of the optimal design solution suggests that the design space search space D_X, should be refined. The current solution is lowly sensitive to the perturbations of the model, which explains that cost and desirability based preference models converge on the same solution. In this context and due to the delays and costs of numerical simulations, we cannot refine our validation process at this stage; this refinement is part of the perspectives of this work.

Other perspectives concern the introduction of new design variables in the design problem, namely alternative technologies in the design of nozzle guide vanes. In particular, we consider alternatives to film cooling such as thermal barrier coating of the blades or the use of multiple ribs, pin-fins or pedestals. These elements would transform the thermal transfers at the surface or inside the blades.

Acknowledgment

The authors wish to thank turbine designers from TURBOMECA SAFRAN Group.

Nomenclature

Lower Case Letters

a,b,c = components of judgement matrix
cx = axial cord,m
$c_1, c_2,\ldots$ = film cooling correlation constants
b_1,b_2, b_3 = models of losses correlation constants
i = increment
m_{fuel} = mass of fuel at take-off, kg
$\dot{m}$ = mass flow, kg/s
oil = low sulphur oil price per barrel, €
s = distance from ejection point, m
u = preference
x = design parameter
y = observation variable
$y+$ = dimensionless wall distance
z = interpretation variable

Upper Case Letters

A = judgement matrix
BL = blowing ratio
Cp = heat capacity at constant pressure, J/kg K
FB = hourly fuel consumption, m^3/h
IA = random index
IC = consistence index
JFP = Jet fuel price, €/m^3
SL = service lifetime, h
M, Mn = Mach number
MPTOW = maximum permissible take-off weight, kg
OEM = operating empty weight, kg
PS = pressure side

RC = consistence ratio
RTDF = radial temperature distribution factor
SS = suction side
T = total temperature, K
Temp = dimensionless total temperature
TVC = aircraft total variable cost, €/h
V = Velocity, m/s
ΔSFC = specific fuel cons. change, Kg/KW/h
ΔPW = output power change, KW

Greek Symbols

α, β = desirability function parameter
δ = desirability
λ_{max} = maximum eigenvalue of A
η = efficiency/effectiveness
ρ_{fuel} = jet A1 density, Kg/m^3
ω = aggregation function weighting

Indexes

40 = combustion chamber exit
41 = high pressure turbine inlet
i = observation variable
n = design variable index
m = observation, interpretation variable index
low = low satisfaction level trigger
high = high satisfaction level trigger

References

[1] Müller, S. D., Walther, J. H., and. Koumoutsakos, P.D., 2000, "Evolution Strategies for Film Cooling Optimization," AIAA J., **39**(3), 537–539.
[2] Nowak, G., and Wroblewski, W., 2009, "Cooling System Optimization of Turbine Guide Vane," Appl. Therm. Eng., **29**, pp. 567–572.
[3] Nowak, G., Wroblewski, W., and Chmielniak, T., 2005, "Optimization of Cooling Passages Within a Turbine Vane," ASME Turbo Expo 2005, Reno, NV, June 6–9, ASME Paper No. GT2005-68552.
[4] Morrone, B., Unich, A., Mariani, A., and De Maio, V., 2009, "Optimization of a Gas Turbine Stator Nozzle Cooling Using Genetic Algorithms," Int. Symp. on Heat Transfer in Gas Turbine Systems, Antalya, Turkey, August 9–14.
[5] Ireland, P., and Dailey, G., 2010, *Aerothermal Performance of Internal Cooling Systems in Turbomachines* (von Karman Lecture Series), von Karman Institute, Rhode-Saint-Genese, Belgium.
[6] Collignan, A., 2011, "Méthode D'Optimisation et D'aide à la Décision en Conception Mécanique: Application à Une Structure Aéronautique," Thèse de Doctorat, Université Bordeaux I, Bordeaux, France.
[7] Sebastian, P., Ledoux, Y., Collignan, A., and Pailhes, J., 2012, "Linking Objective and Subjective Modeling in Engineering Design Through Arc-Elastic Dominance," Expert Systems With Applications, **39**(9), pp. 7743–7756.
[8] Antonsson, E. K., and Otto K. N., 1995, "Imprecision in Engineering Design," ASME J. Mech. Des., **117**, pp. 25–32.
[9] Schmidt, R. C., and Patankar, S. V., 1991, "Simulating Boundary Layer Transition With Low Reynolds Number k-ε Turbulence Models," ASME J. Turbomach., **113**(1), pp. 10–26.
[10] Sibulkin, M., 1952, "Heat Transfer Near the Forward Stagnation Point of a Body of Revolution," J. Aeronaut. Sci., **19**(8), pp. 570–571.
[11] Xing, Y., Spring, S., and Weigand, B., 2010, "Experimental and Numerical Investigation of Heat Transfer Characteristics of Inline and Staggered Arrays of Impinging Jets," ASME J. Heat Transfer, **132**(9), p. 092201.
[12] Haselbach, F., 2008, "HP Turbine Design," *Aero-Engine Design: Form State of the Art Turbofans Towards Innovative Architectures* (von Karman Lecture Series), von Karman Institute, Rhode-Saint-Genese, Belgium.
[13] Cambier, L., and Veuillot, J. P., 2008, "Status of the elsA CFD Software for Flow Simulation and Multidisciplinary Applications," AIAA Paper No. 2008-664.
[14] Hartsel, J. E., 1972, "Prediction of Effects of Mass-Transfer Cooling on the Blade Row Efficiency of Turbine Airfoils," ASME Paper. No. 72-11.
[15] Sallee, G. P., 1978, "Performance Deterioration Based on Existing (Historical) Data, JT9D Jet Engine Diagnostics Program," Paper No. NASA-CR-135448.
[16] Newell, R., 2010, "Annual Energy Outlook 2011 Reference Case," US Energy Information Administration, Washington, DC.
[17] Sikorsky S-76C++™ Helicopter, Executive Transport Technical Information, 2007, Sikorsky Aircraft Corporation, Stratford, CT.
[18] "Offshore Rig Utilization by Region," 2012, http://www.rigzone.com.
[19] Conklin & de Decker Aviation Information, 2012, available at http://www.conklindd.com
[20] Harrington, E. C., 1965, "The Desirability Function," Industrial Quality Control, **21**, pp 494–498.
[21] Derringer, G., and Suich, R., 1980, "Simultaneous Optimization of Several Response Variables," J. Quality Technol., **12**(4), pp. 214–219.
[22] Scott, M. J., and Antonsson, E.K., 1995, "Aggregation Functions for Engineering Design Trade-Offs," 9th International Conference on Design Theory and Methodology, Boston, MA, September 17–20, Vol. 2, pp. 379–396.
[23] Scott, M. J., and Antonsson, E.K., 1998, "Aggregation Functions for Engineering Design Trade-Offs," Fuzzy Sets Syst., **99**(3), pp 253–264.
[24] Messac, A., Puemi-Sukam, C., and Melachrinoudis, E., 2000, "Aggregate Objective Functions and Pareto Frontiers: Required Relationships and Practical Implications," Optim. Eng., **1**, pp. 171–188.
[25] Saaty, T. L., 2008, "Relative Measurement and Its Generalization in Decision Making Why Pairwise Comparisons are Central in Mathematics for the Measurement of Intangible Factors the Analytic Hierarchy/Network Process," Real Academia de Ciencias, **102**(2), pp. 251–318.
[26] Noesis Solutions, 2010, "OPTIMUS Theoretical Background," Leuven, Belgium.